The Inner 25 au Debris Distribution in the ε Eri System

Kate Y. L. Su (University of Arizona)

J. De Buizer, G. H. Rieke, A. Krivov, T. Lohne, M. Marengo, K. R. Stapelfeldt, N. Ballering, W. Vacca

2017, AJ, 153, 226

3a, 4-13-17, LCook

Definition of Debris Disks

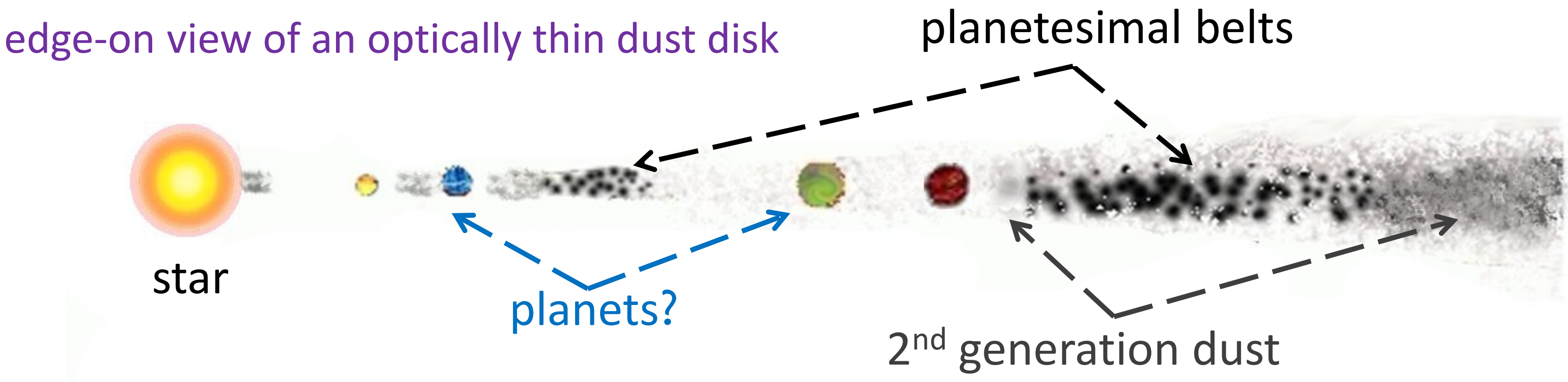

- dust replenished by collisions or cometary activity
- leftover ~km-size planetesimals that failed to form planets

• The large surface area of a dusty disk makes it readily observable in Infrared, and optical scattered light in favored conditions.

• The gravity of giant planets determines where leftover planetesimal belts can exist, stirs up collisions in the belts, and sculpts the dust distribution through resonant and secular interactions.

Great Facilities to Study Planetary Debris Disks

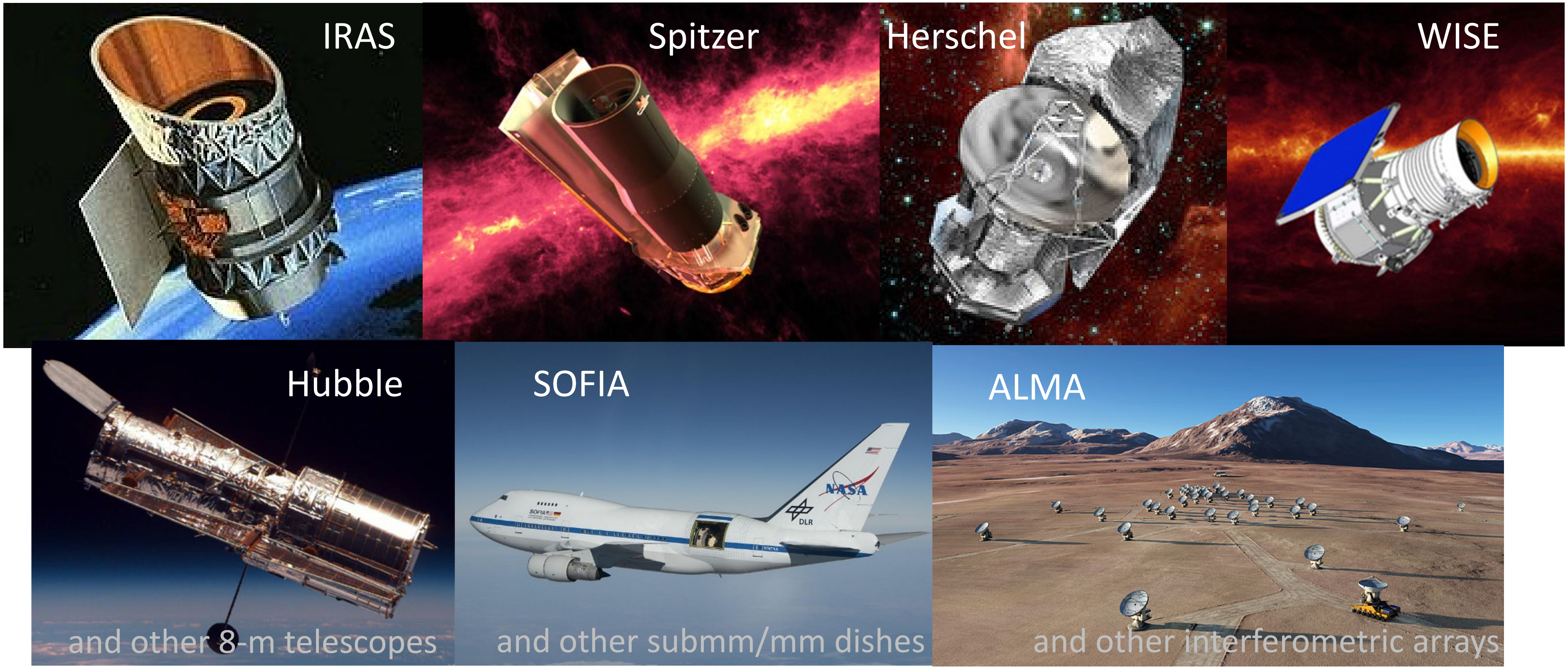

- More than ~400 debris disks known within ~100 pc.
- Small (μm-size) particles dominate the disk opacity and large (>>100 μm-size) particles dominate the mass
- Most disks are unresolved (only a few dozens are resolved) with broad-band Spectral Energy Distributions (SEDs) to determine global dust temperatures

Known Debris Disks are the Tip of the Iceberg

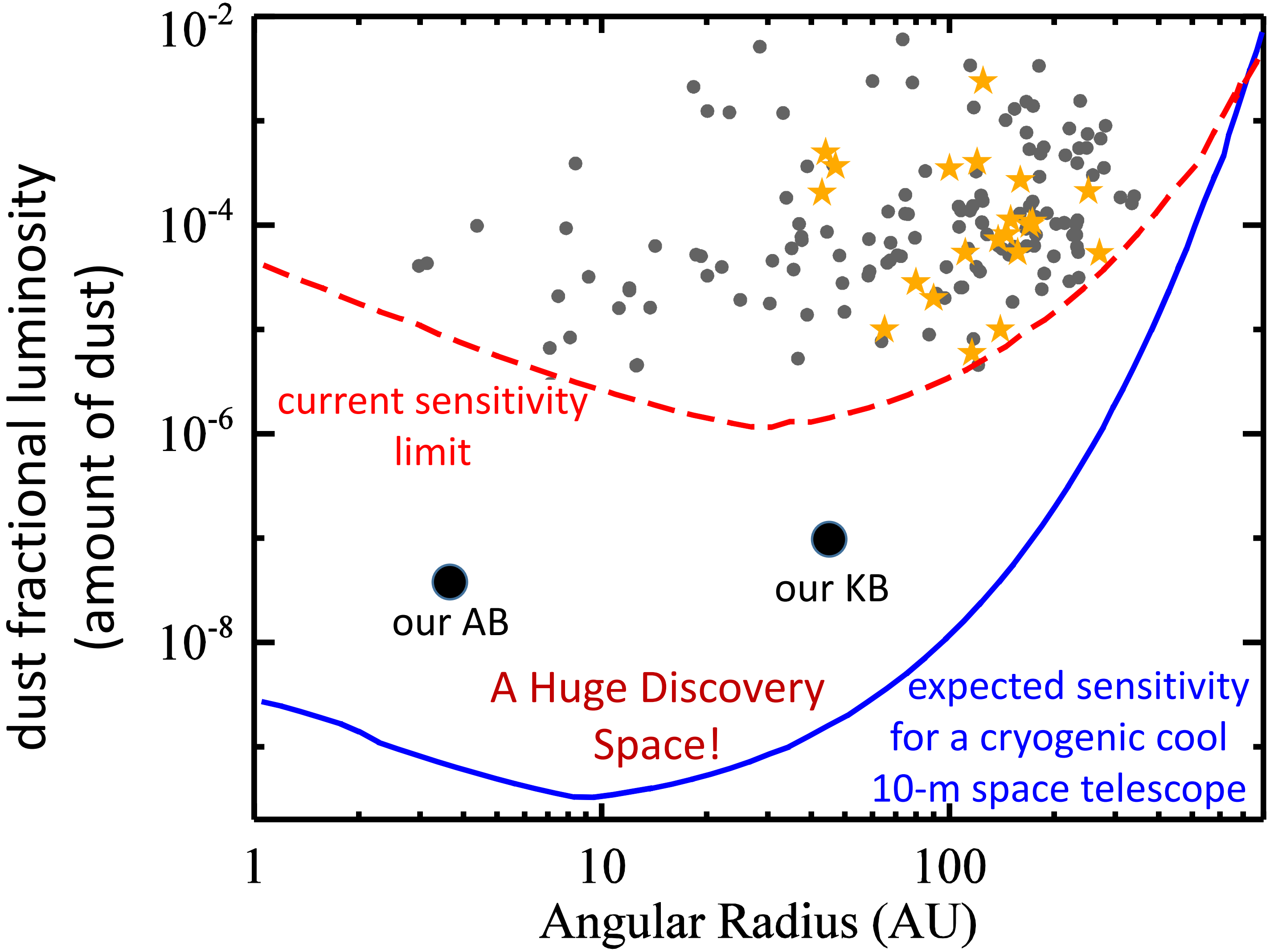

A large, cryogenic cold telescope (like OST) can discover many more disks, and provide a census of true KB analogs, putting our SS into context.

Prototype – the Fomalhaut System

- Fomalhaut: A3V, 7.7pc, 440±40 Myr
- Its proximity and luminosity make its structure easily resolved.

IRAS
1984

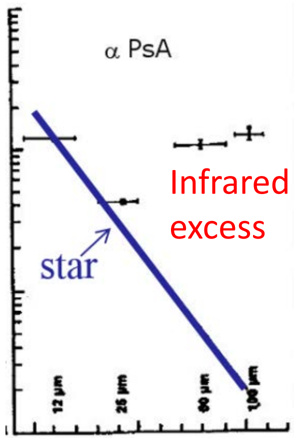

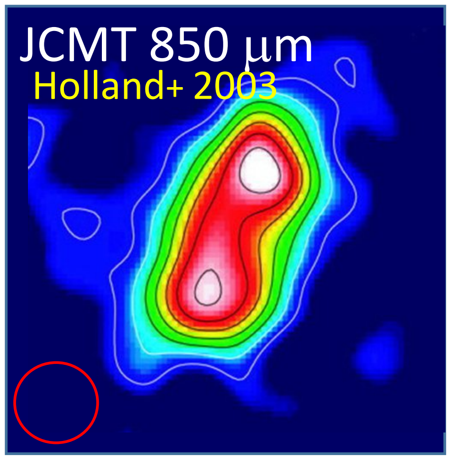

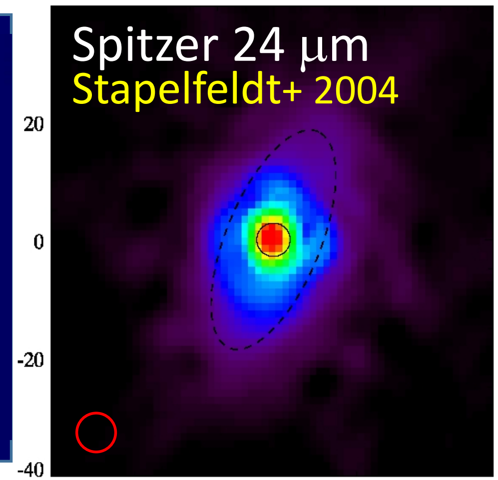

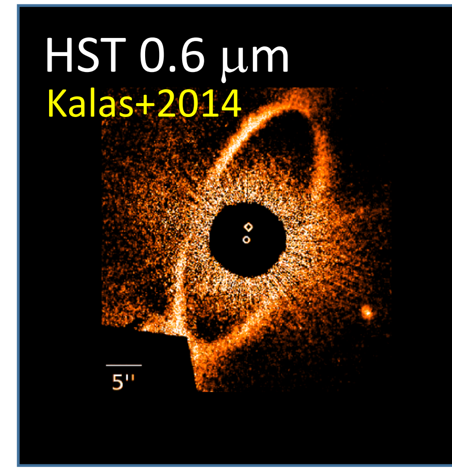

VLTI/VLT K-band

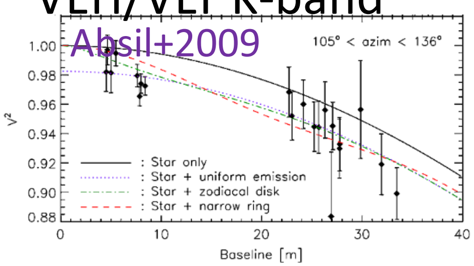

KIN N-band

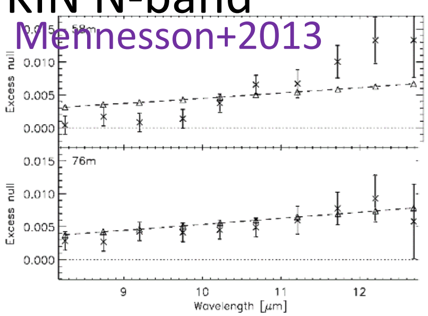

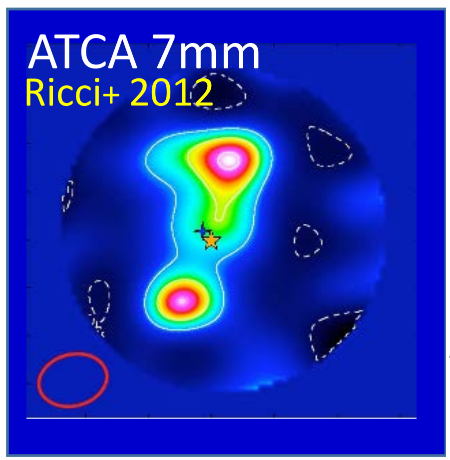

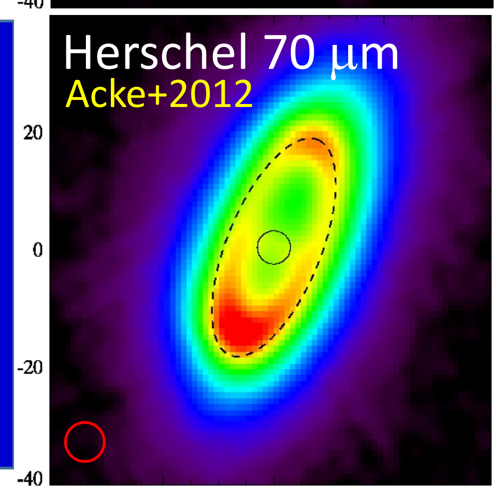

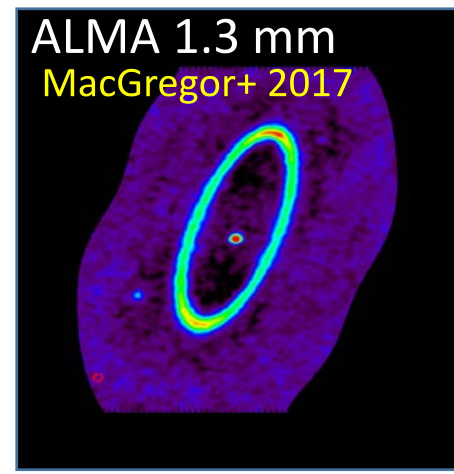

A wealth of observations at a wide range of wavelengths and spatial scales from photometry, imaging to interferometry!

Dust Zones Revealed by Great Observatories

edge-on view of nearby **planetary debris disks** → distance, r, increases

← *dust temperature*, $T_d \sim \frac{1}{\sqrt{r}}$

~1500 K very hot dust

~500 K hot dust

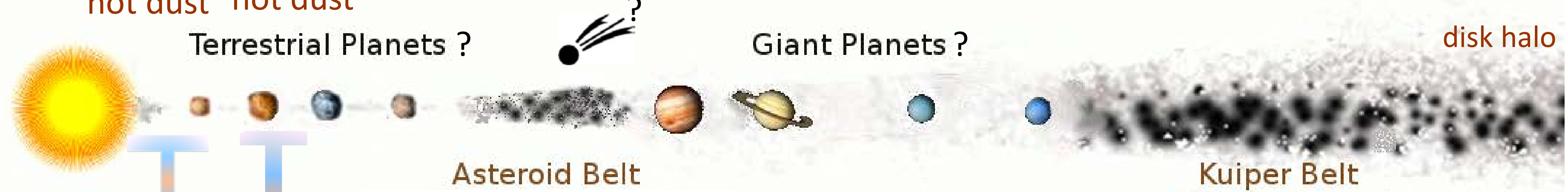

~150 K warm dust

~50 K cold dust

probed by NIR 2 μm interferometry

probed by MIR 8-13 μm interferometry, Spitzer, WISE and SOFIA

probed by Spitzer, SOFIA, Herschel, and ALMA

probed by Spitzer, SOFIA, Herschel, HST, and ALMA

distance not to scale

2 μm ~10 μm ~24-35 μm ~60-70 μm

→ peak wavelength of emission

Su & Rieke 2014

Planetary Architecture of Solar System & ε Eri

Solar System G2V star, 4.5 Gyr

ε Eri System K2V star, ~800 Myr
3.22 pc (or 10.5 yr)

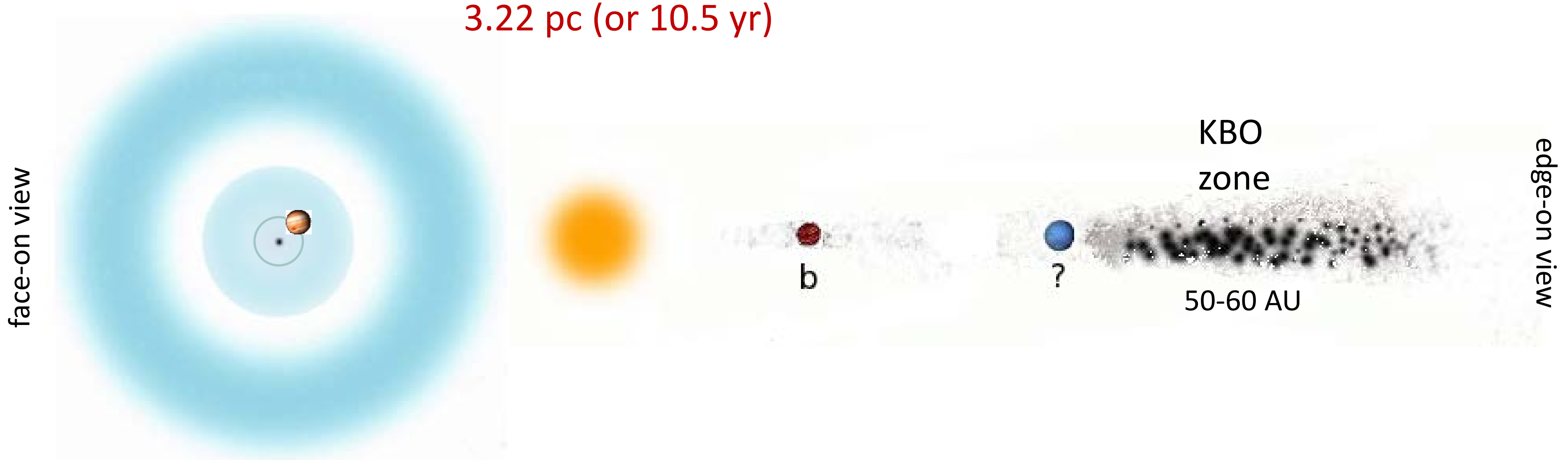

Planetary Architecture of Solar System & ε Eri

Solar System G2V star, 4.5 Gyr

ε Eri System K2V star, ~800 Myr
3.22 pc (or 10.5 yr)

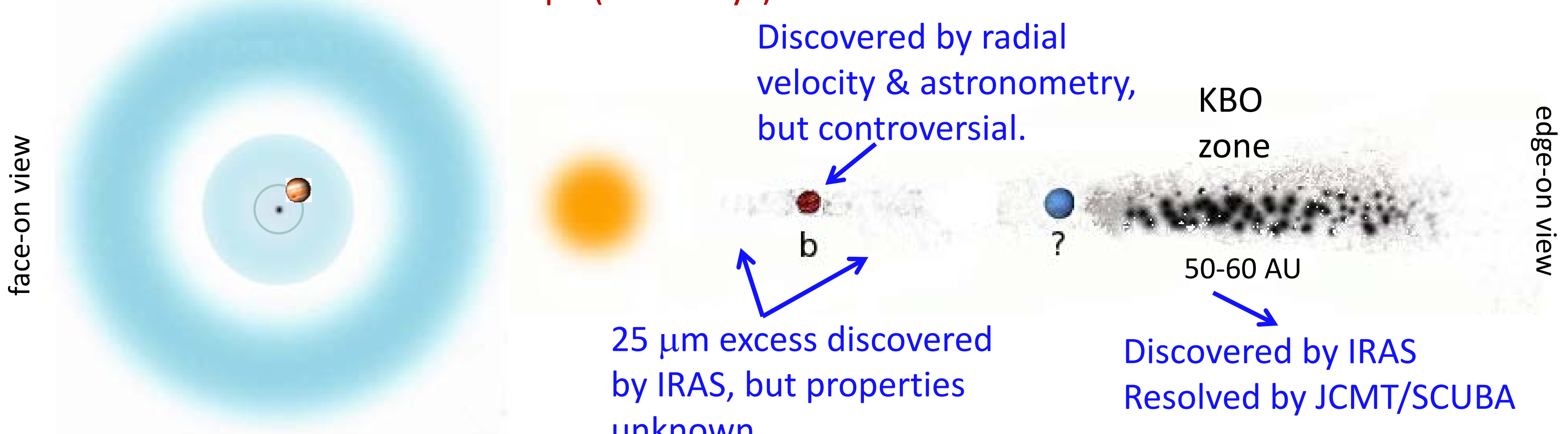

Planetary Architecture of ε Eri

In addition to the KBO-like belt discovered by IRAS in 1984, Backman et al. 2009, based on data obtained from Spitzer, suggest two inner belts interior to the cold belt.

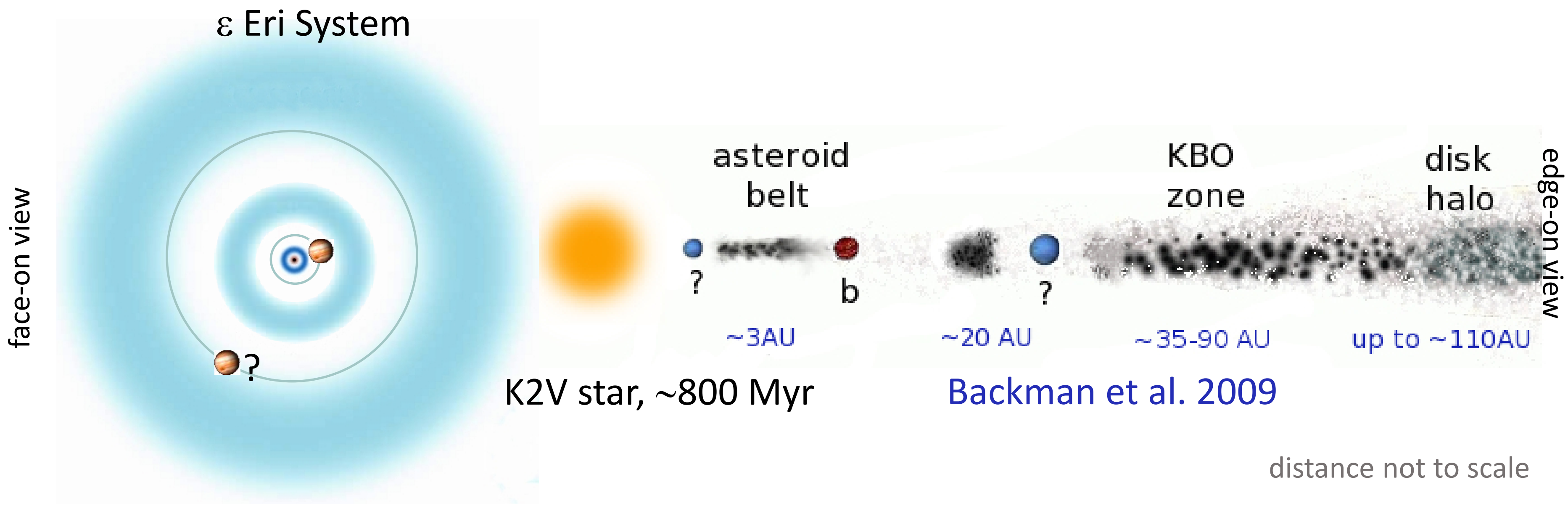

Planetary Architecture & Debris Distribution

Planets determine the debris distribution in a planetary system. Dust debris also influences by non-gravitational forces, and their resultant emission is temperature dependent.

- Particle Distribution for Solar System

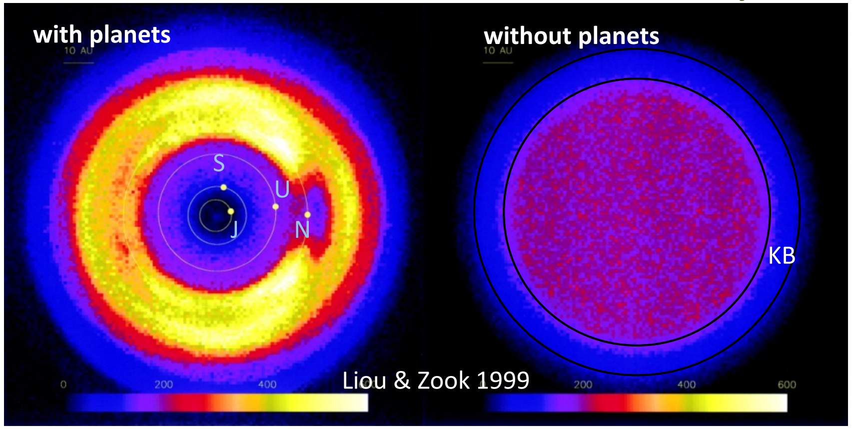

Planetary Architecture & Debris Distribution

Planets determine the debris distribution in a planetary system. Dust debris also influences by non-gravitational forces, and their resultant emission is temperature dependent.

- Particle Distribution for Solar System

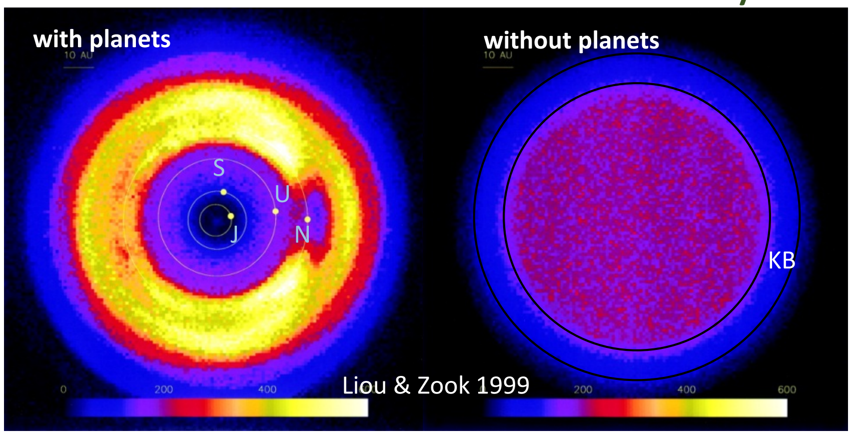

- Mid-Infrared Emission Distribution

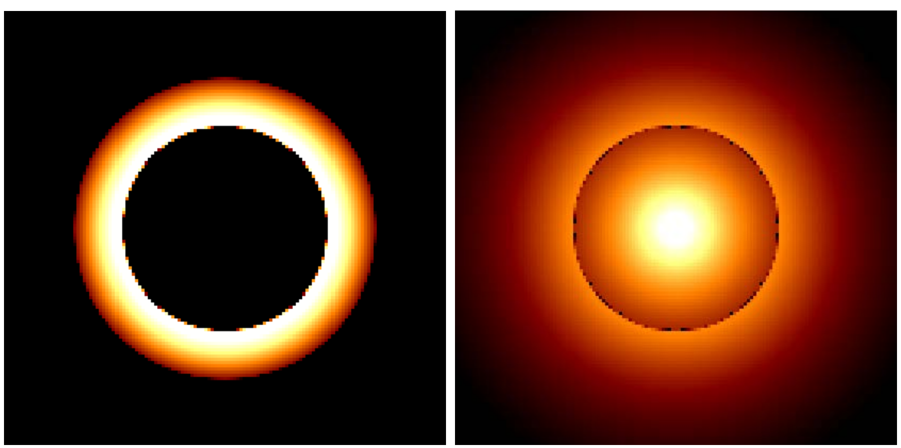

one belt w/ planets one belt w/o planet

Warm Belts vs. Dragged-in Grains

Planets determine the debris distribution in a planetary system. Dust debris also influences by non-gravitational forces, and their resultant emission is temperature dependent.

- Particle Distribution for Solar System

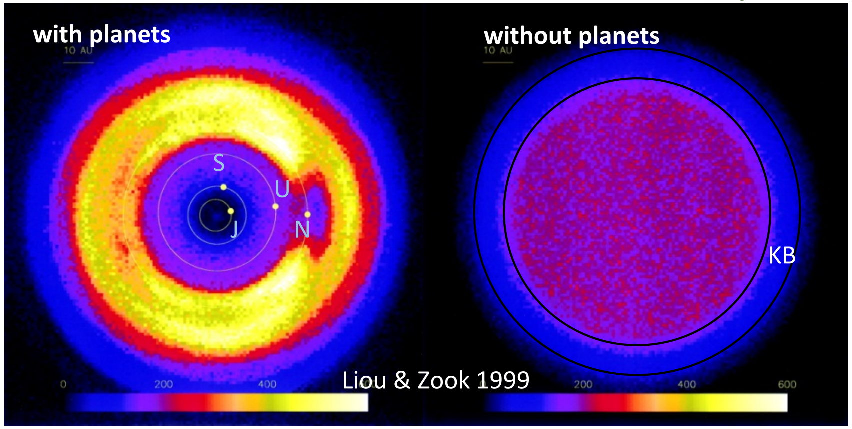

Liou & Zook 1999

- Mid-Infrared Emission Distribution

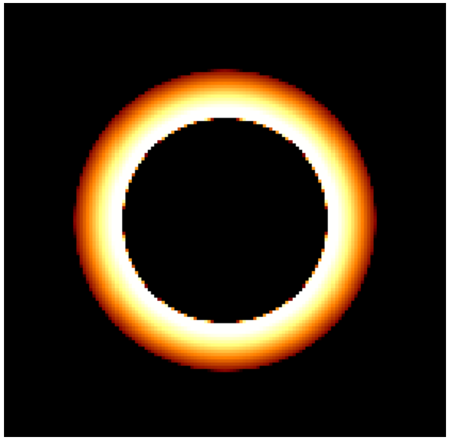

one belt w/ planets

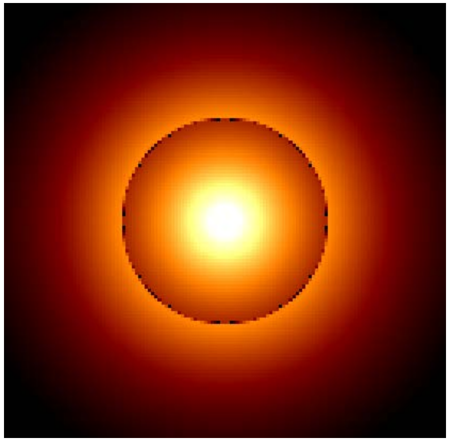

one belt w/o planet

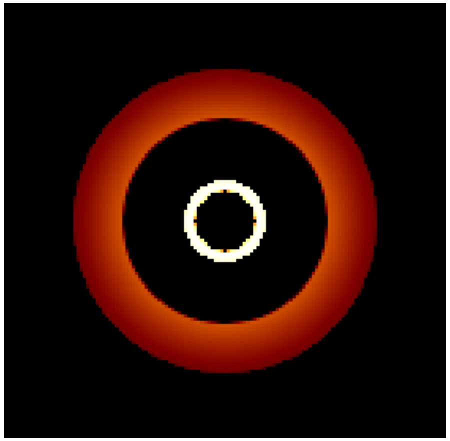

two belts w/ planets

Warm Belts vs. Dragged-in Grains

Planets determine the debris distribution in a planetary system. Dust debris also influences by non-gravitational forces, and their resultant emission is temperature dependent.

- Particle Distribution for Solar System

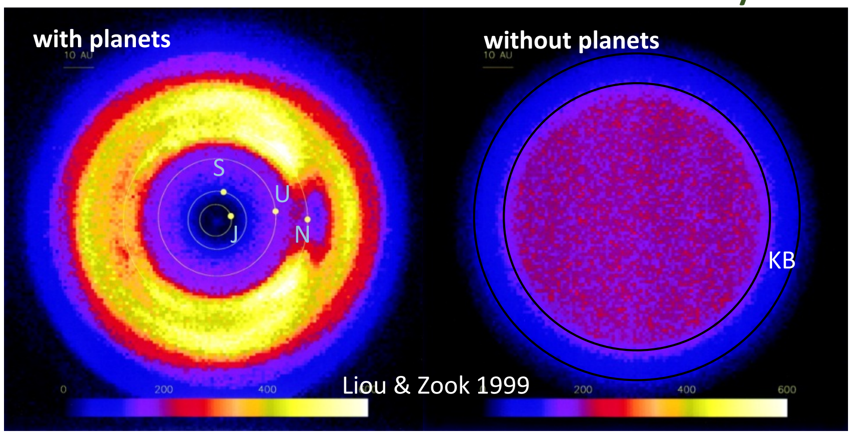

- Mid-Infrared Emission Distribution

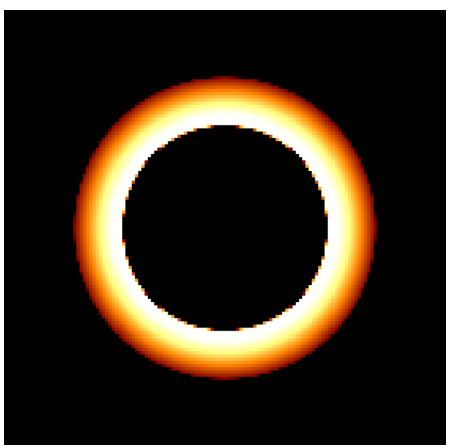

one belt w/ planets

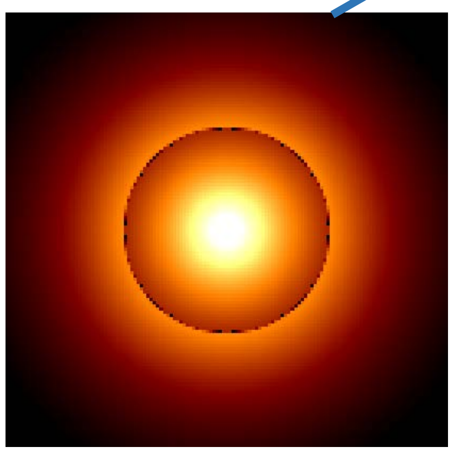

one belt w/o planet

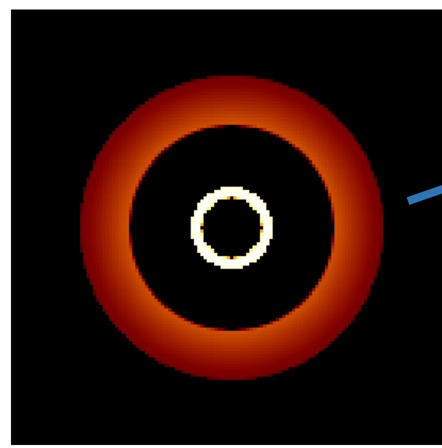

two belts w/ planets

Warm Belts vs. Dragged-in Grains

Based on marginally resolved mid- and far-infrared images and SED, two publications propose totally different explanations for the warm excess in ε Eri:

Backman et al. 2009

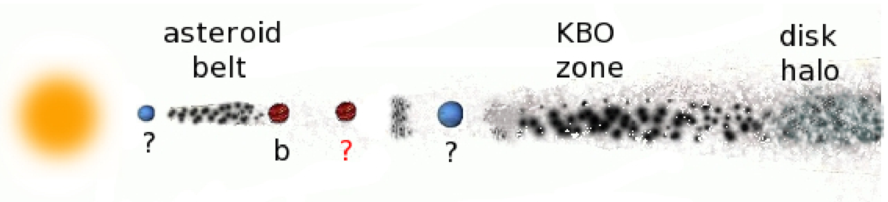

Two warm belts + One cold belt

Implication: existence of multiple planets

Reidemeister et al. 2011

One cold belt + small grains being transported inward by P-R and stellar wind drags

Implication: one or no planet is ok

Warm Belts vs. Dragged-in Grains

Based on marginally resolved mid- and far-infrared images and SED, two publications propose totally different explanations for the warm excess in ε Eri:

Backman et al. 2009

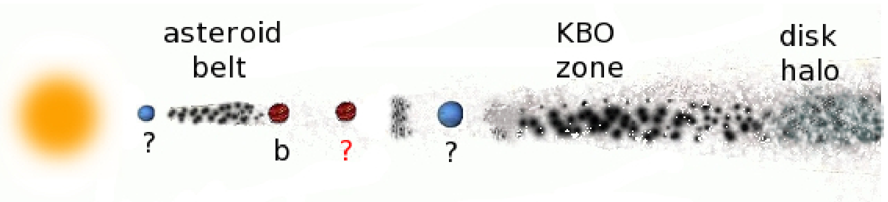

Two warm belts + One cold belt

Implication: existence of multiple planets

Reidemeister et al. 2011

One cold belt + small grains being transported inward by P-R and stellar wind drags

Implication: one or no planet is ok

prediction for SOFIA 35 μm

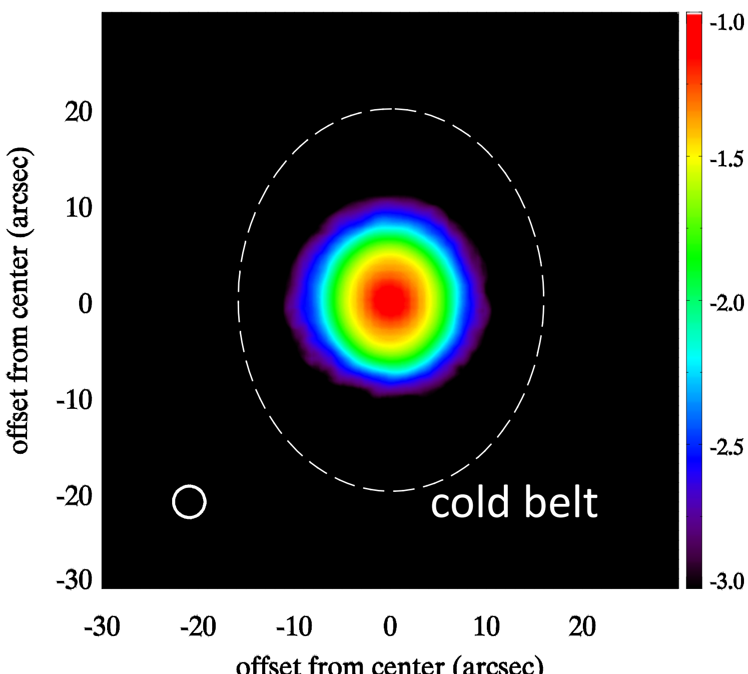

noiseless model images

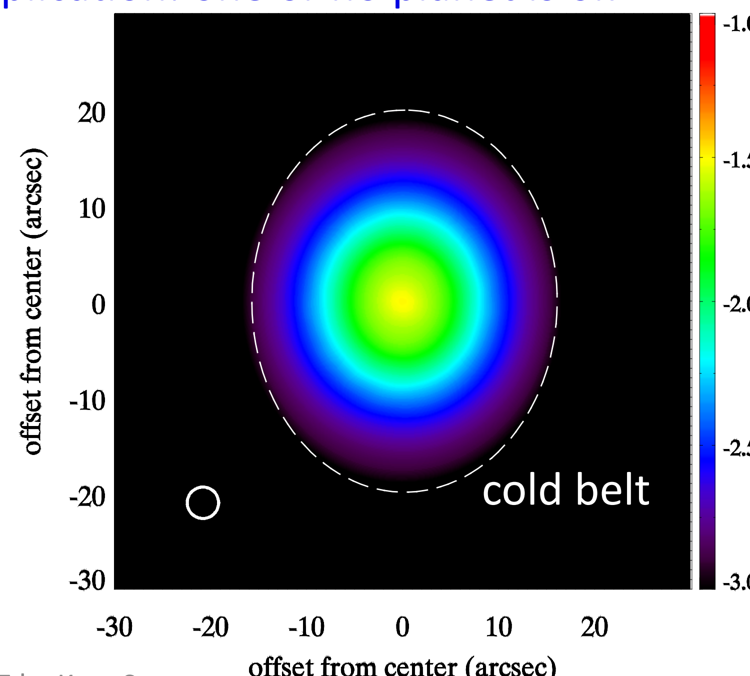

SOFIA/FORCAST Observation of ε Eri

#	Flight	Date	UT Time	FWHMx [arcsec]	FWHMy [arcsec]	σ_{sky} [mJy arcsec^{-2}]	Integration† [sec]
1	190	2015-01-29	05:02:38.8	4.51	3.15	6.64	1162
2	190	2015-01-29	05:29:09.6	4.32	3.48	5.75	1290
3	190	2015-01-29	05:59:43.5	4.26	3.43	6.37	1162
4	190	2015-01-29	06:25:51.9	3.53	3.11	7.10	1032
5	190	2015-01-29	06:52:34.9	3.64	3.28	6.21	1162
6	190	2015-01-29	07:19:24.5	4.60	2.64	7.26	774
7	191	2015-02-04	04:08:12.2	4.42	3.77	6.58	1678
8	191	2015-02-04	04:36:37.4	3.57	3.26	7.11	1420
9	254	2015-11-04	06:44:39.5	3.79	3.57	2.69	4368
10	258	2015-11-13	06:32:55.6	4.70	3.91	3.12	4048

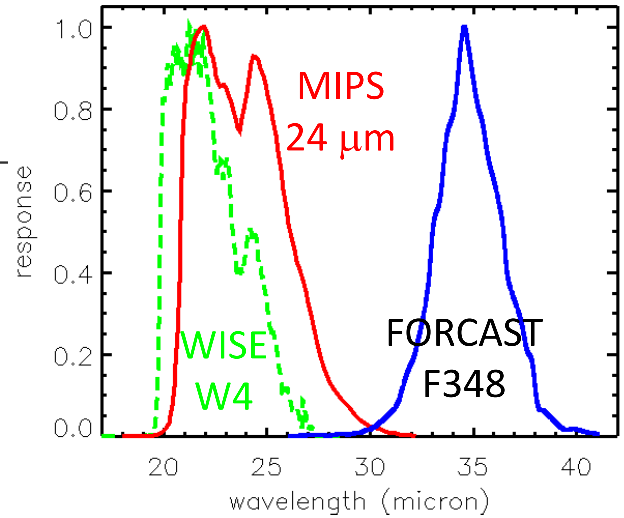

- Data Obtained in SOFIA Cycle 2/3
- FORCAST + F348 filter

  λ_{eff}=34.8 μm   Δλ=3.8 μm

  3.4'x3.8' f.o.v.   0.768"/pixel

  Resolution = 3.4" (11 AU @ε Eri)
- A total of 5 hours on-source integration.

PSF Characterization

MIPS 24 μm PSF

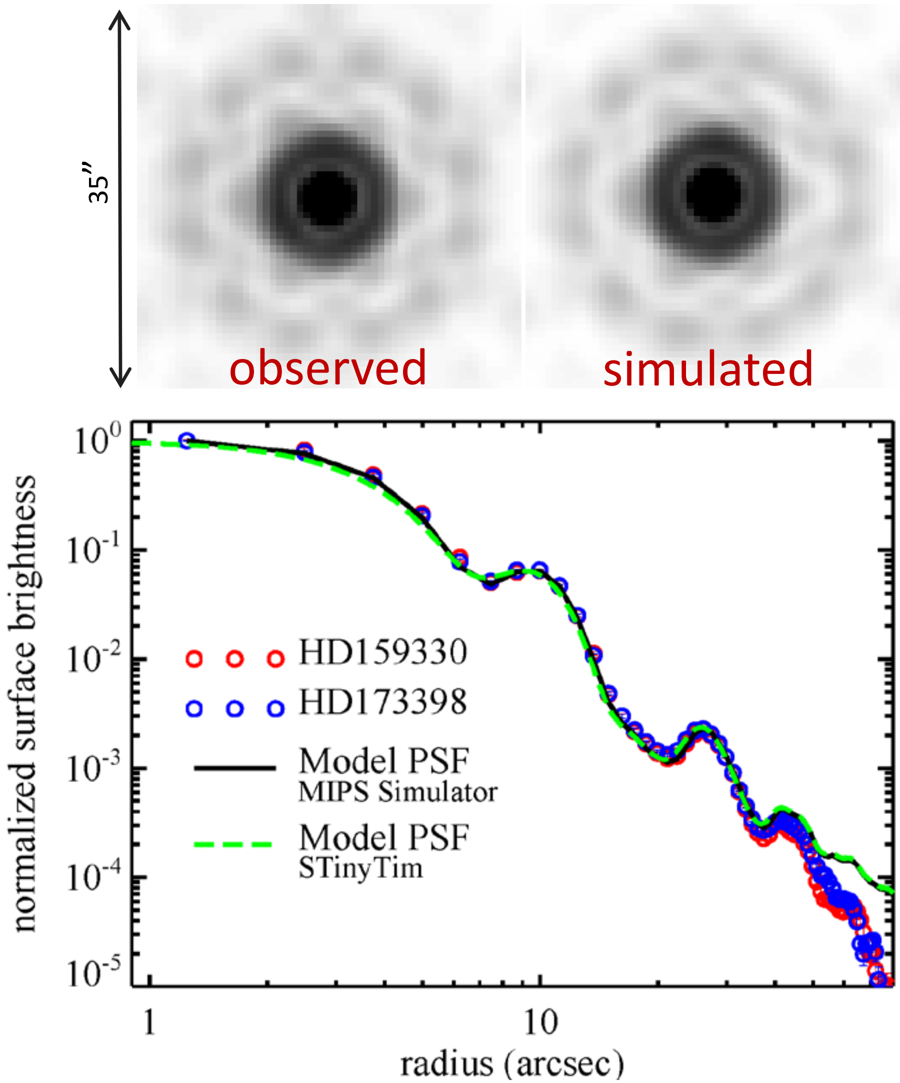

PSF Characterization

MIPS 24 μm PSF

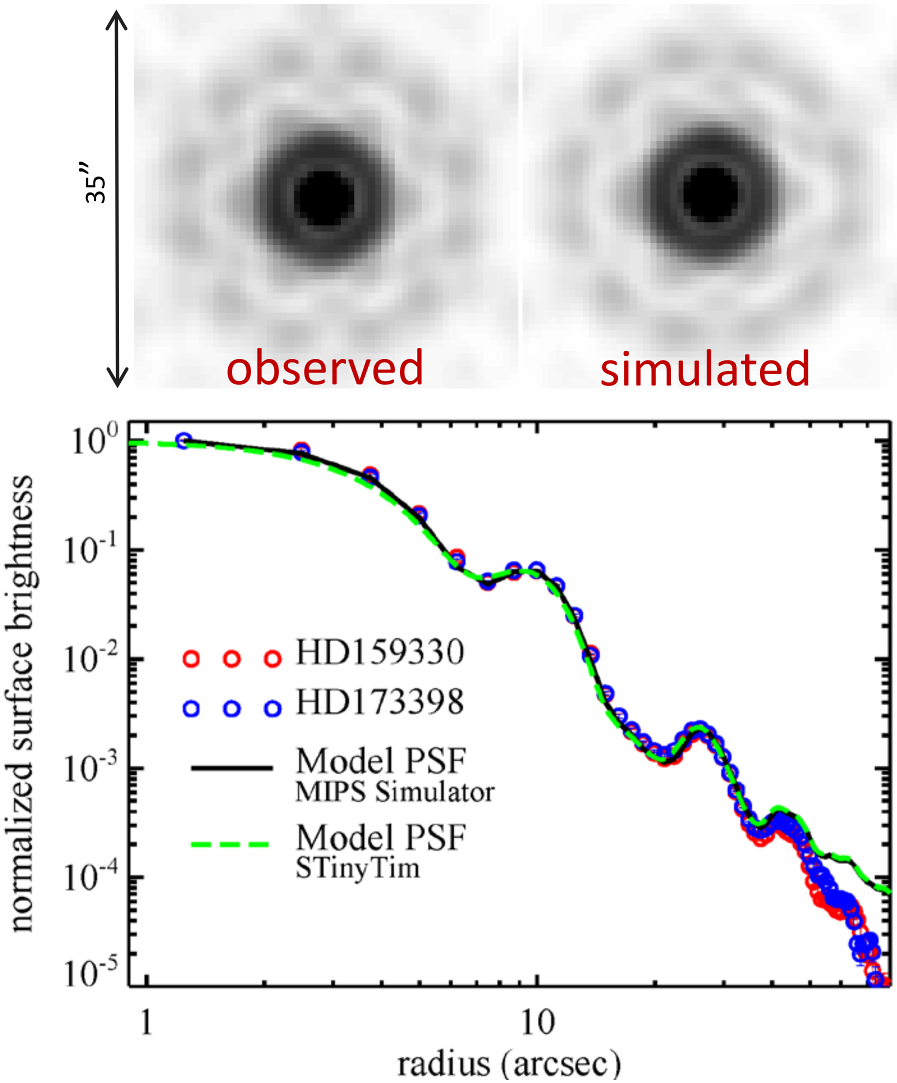

FORCAST 35 μm PSF

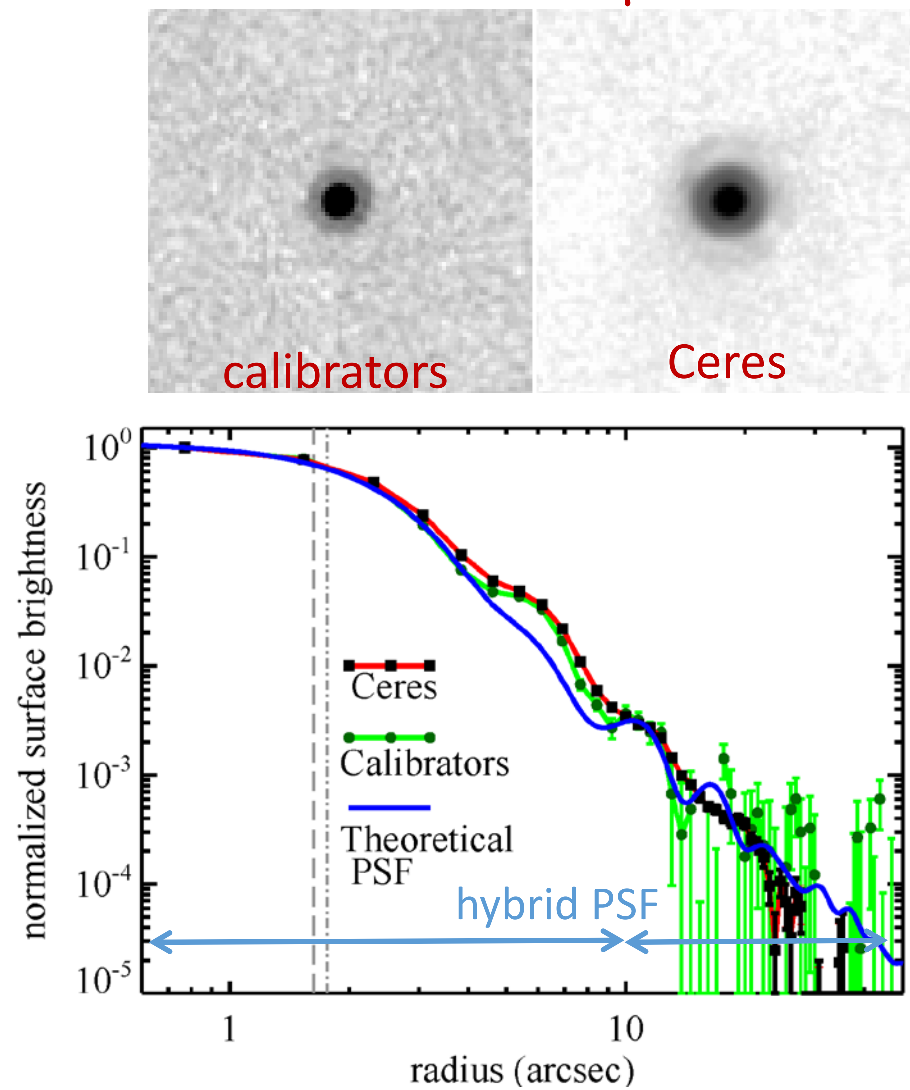

FORCAST Observation of the ε Eri Debris Disk

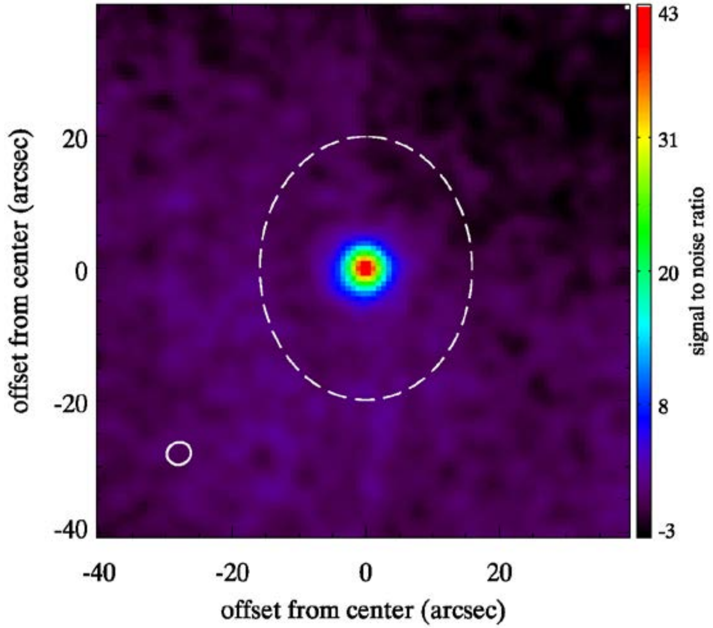

The star dominates the flux at 35 μm, which is detected at S/N of ~40.

FORCAST Observation of the ε Eri Debris Disk

Star subtracted 35 μm image

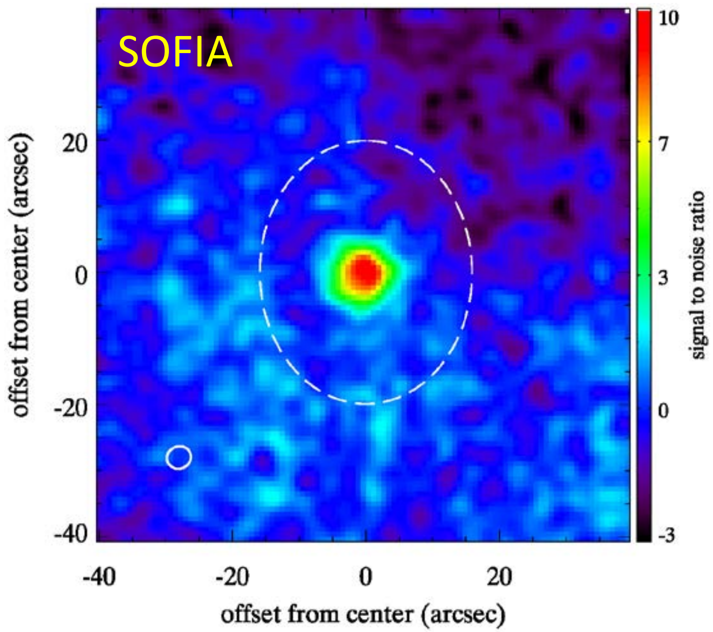

Stellar Calibrators 35 μm

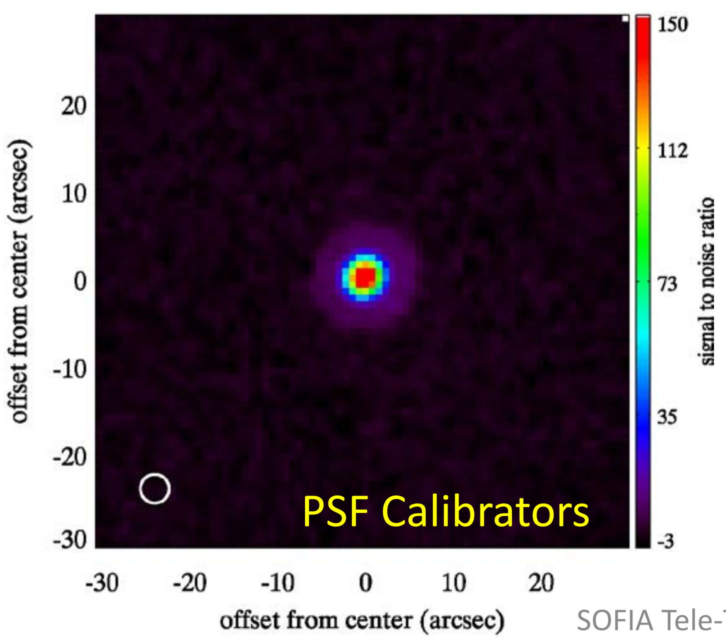

FORCAST Observation of the ε Eri Debris Disk

Star subtracted 35 μm image

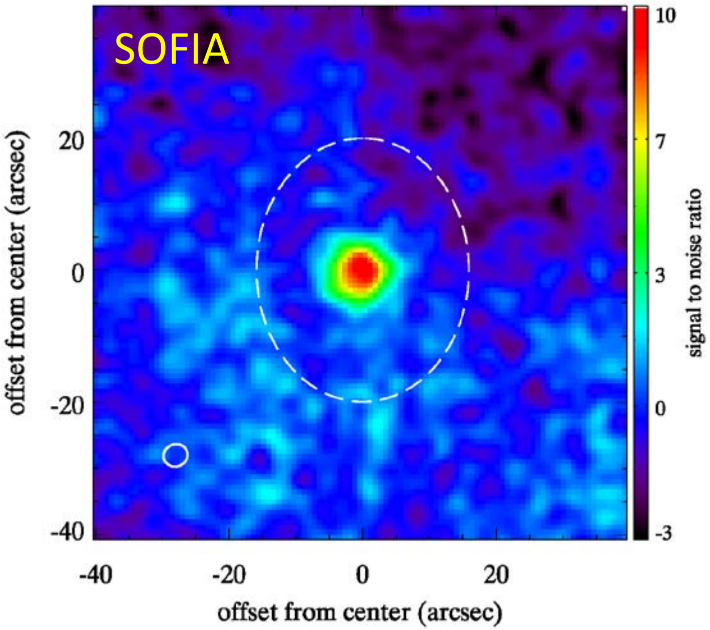

LMT 1 mm image

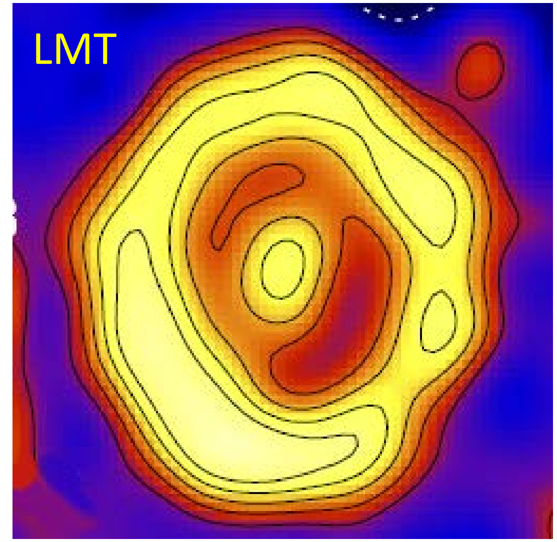

mm image shows the location of the cold belt. Chavez-Dagostino et al. 2016

Stellar Calibrators 35 μm

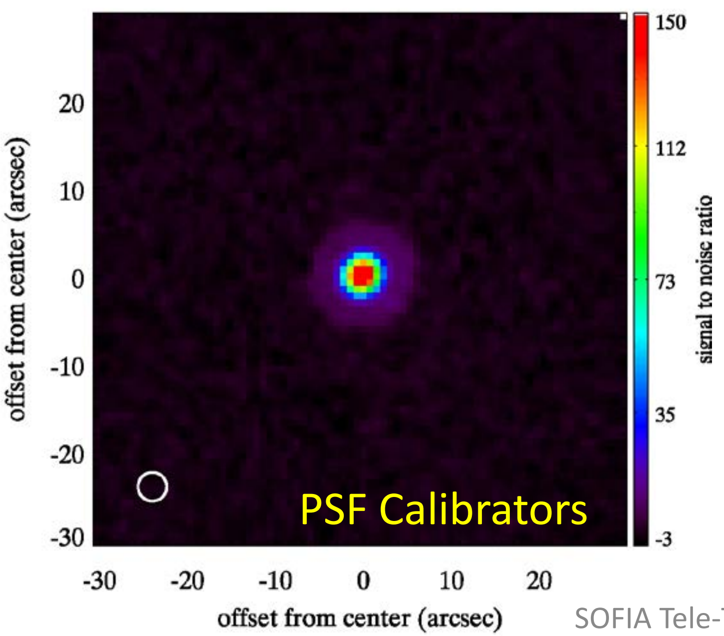

FORCAST Observation of the ε Eri Debris Disk

Star subtracted 35 µm image

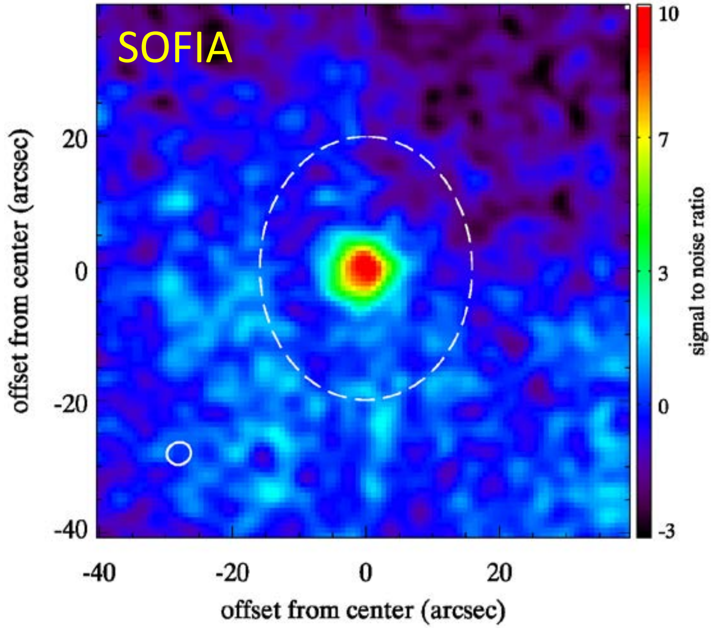

LMT 1 mm image

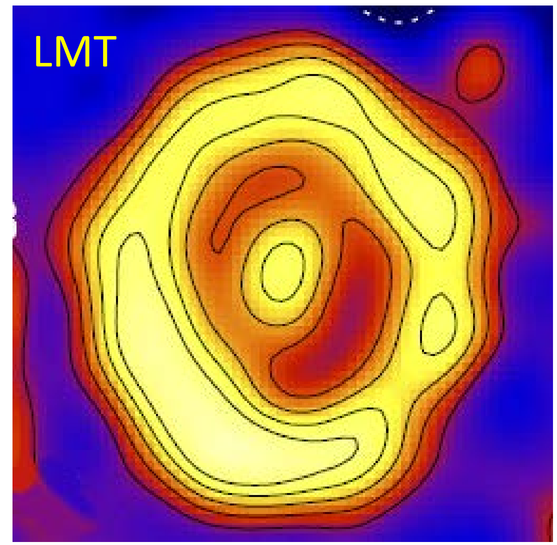

mm image shows the location of the cold belt. Chavez-Dagostino et al. 2016

Stellar Calibrators 35 µm

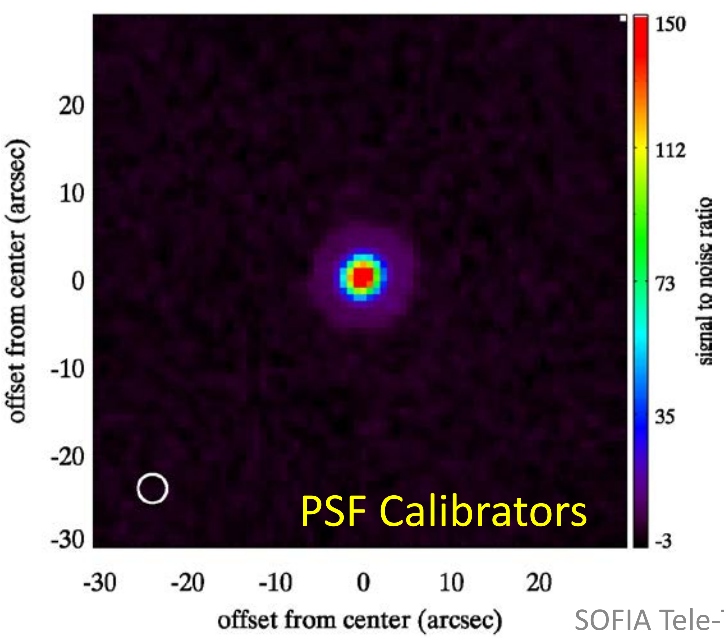

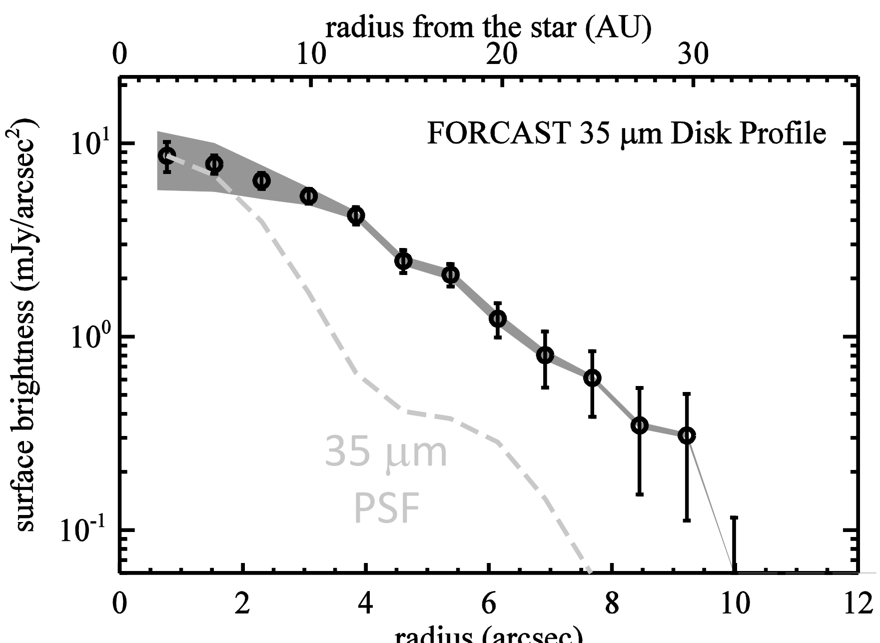

Warm Belts vs. Dragged-in Grains

Model I:

Two warm belts + One cold belt

Implication: existence of multiple planets (Backman et al. 2009)

Model II:

One cold belt + small grains being transported inward by P-R and stellar wind drags

Implication: one or no planet is ok (Reidemeister et al. 2011)

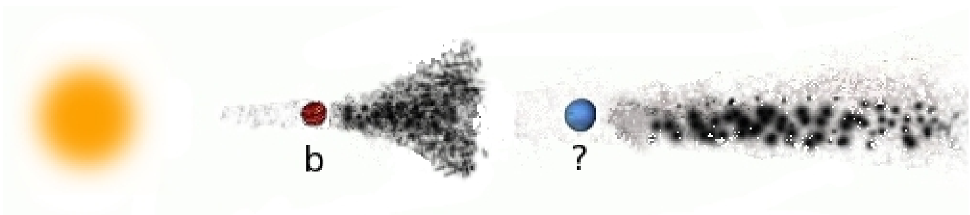

Model III:

One broad disk + One cold belt

Implication: existence of >= two planets (Greaves et al. 2014)

Data Used to Test Models

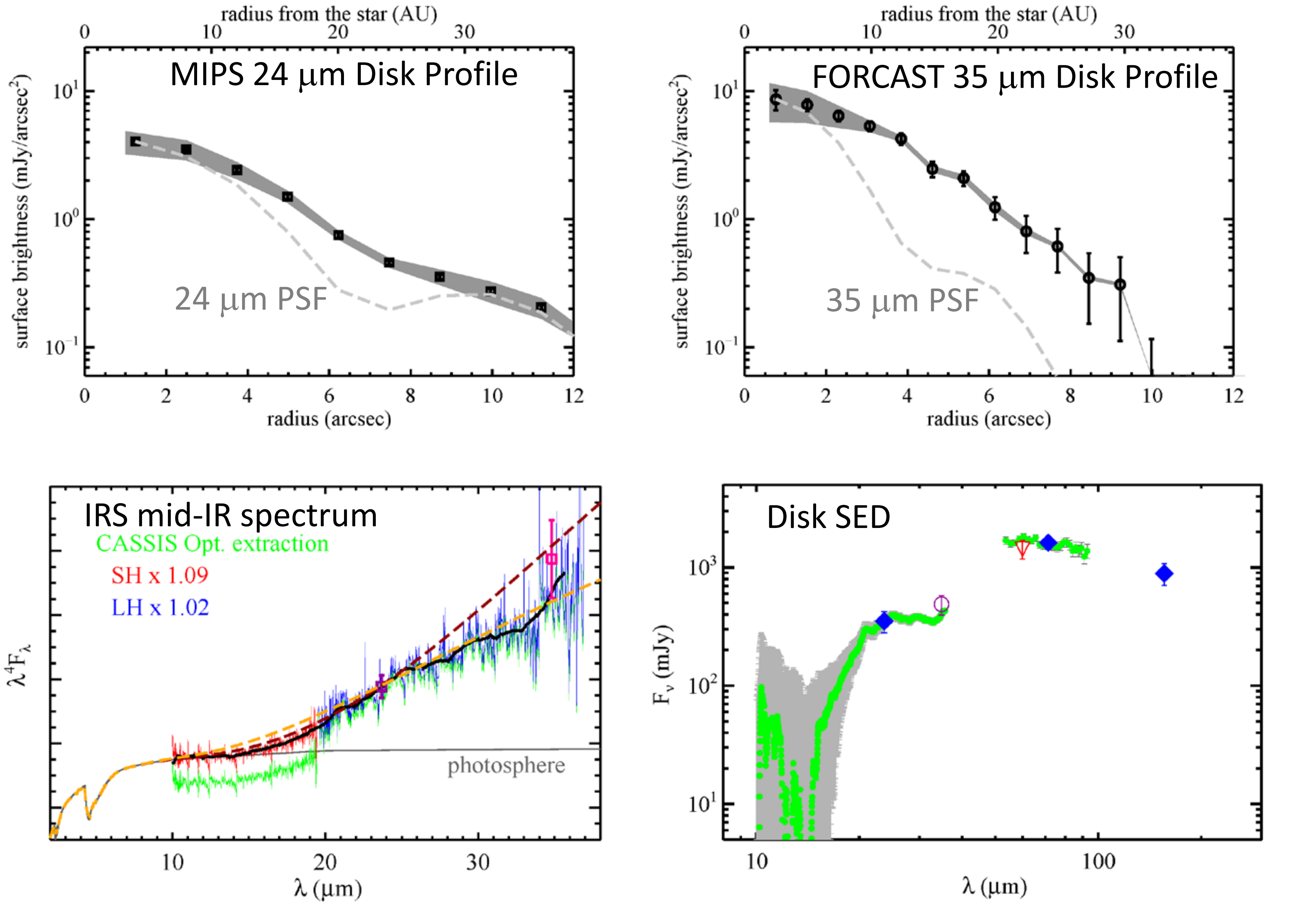

Warm Belts vs. Dragged-in Grains

Model I: Two warm belts + One cold belt

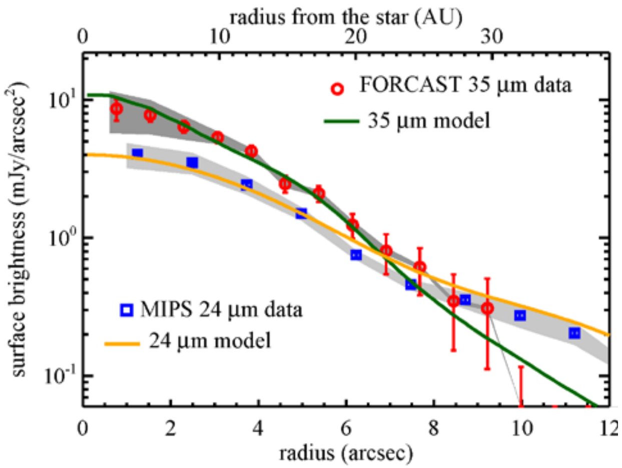

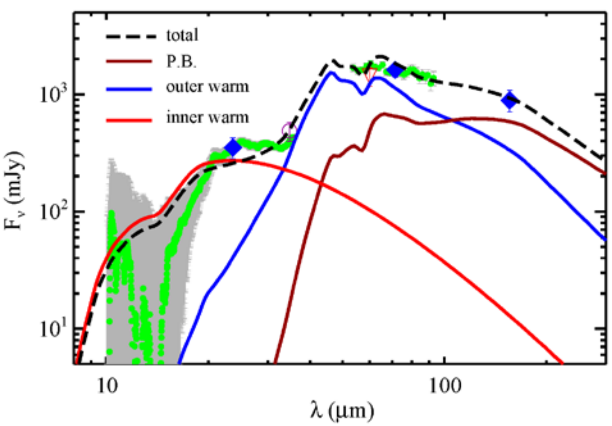

Model II: Dragged-in grains + One cold belt

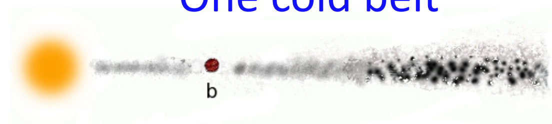

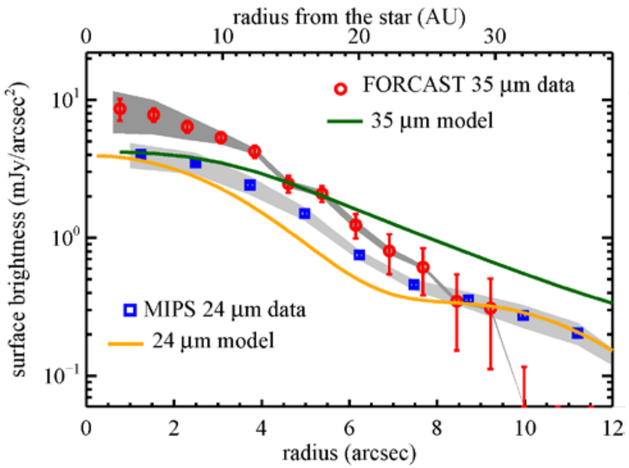

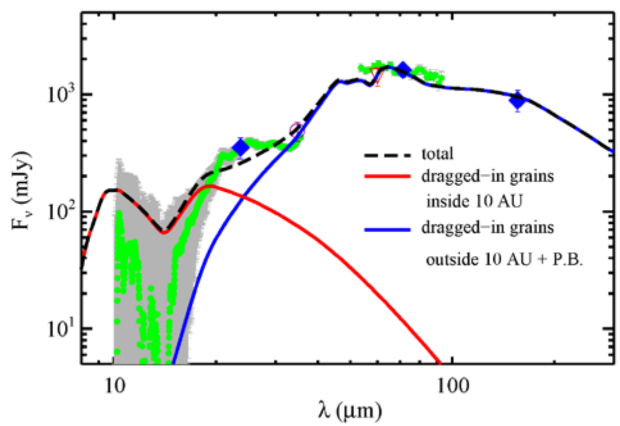

Model III: One warm broad disk + One cold belt

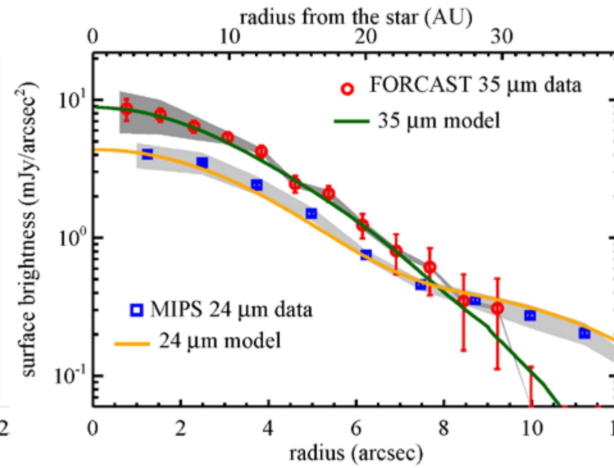

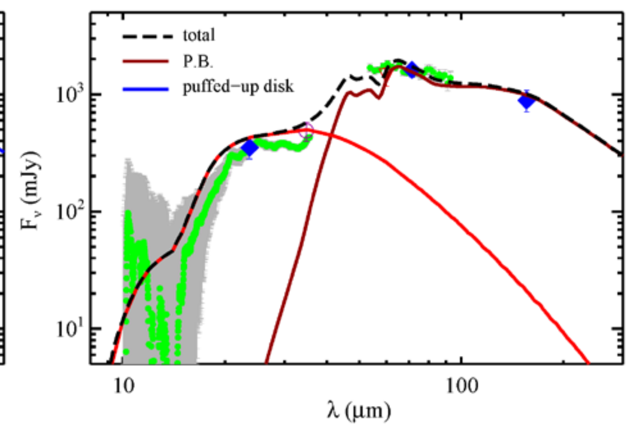

Warm Belts vs. Dragged-in Grains

Model I: Two warm belts + One cold belt

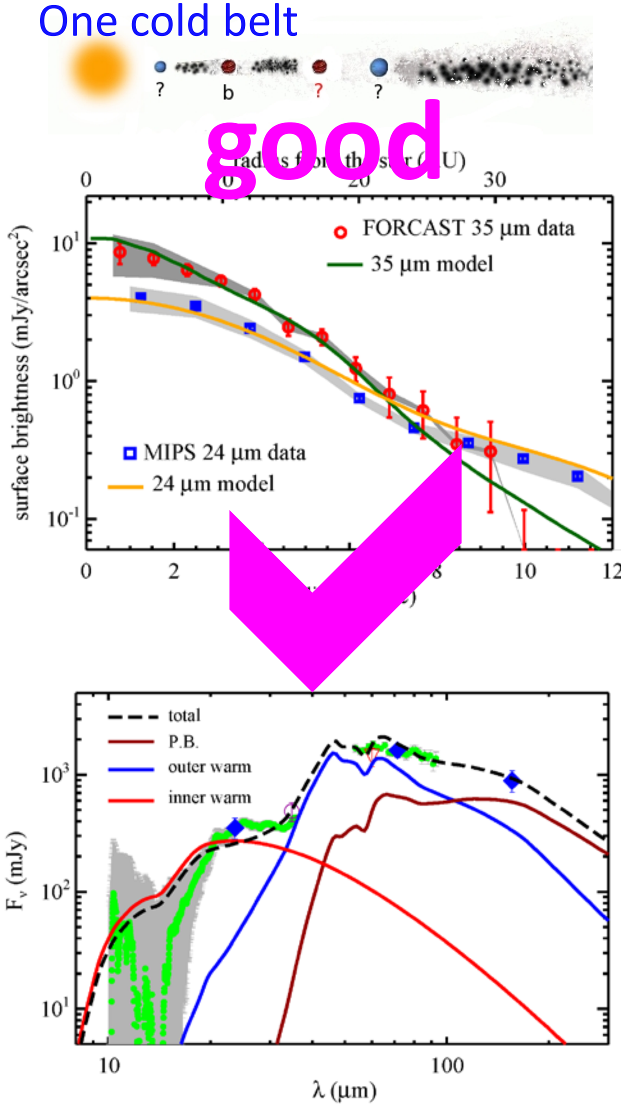

Model II: Dragged-in grains + One cold belt

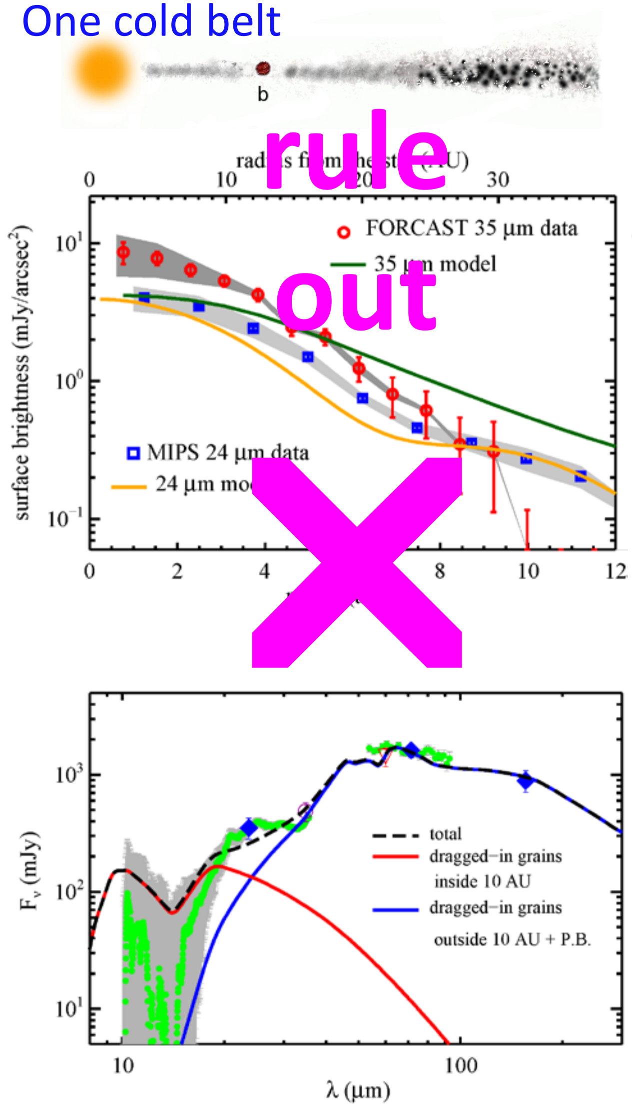

Model III: One warm broad disk + One cold belt

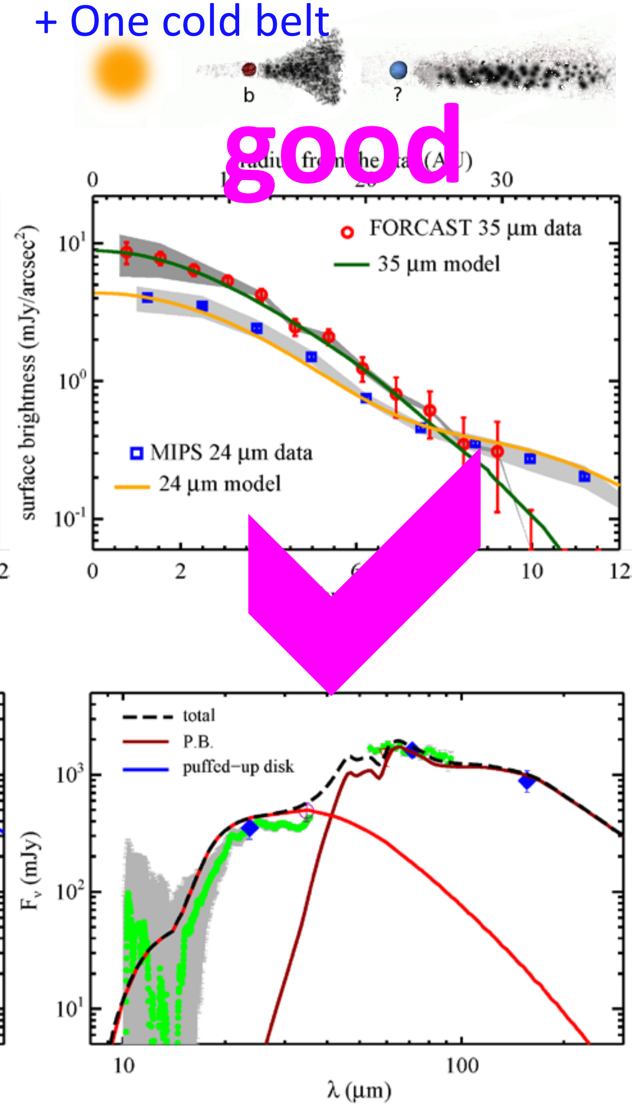

FORCAST Observation of the ε Eri Debris Disk

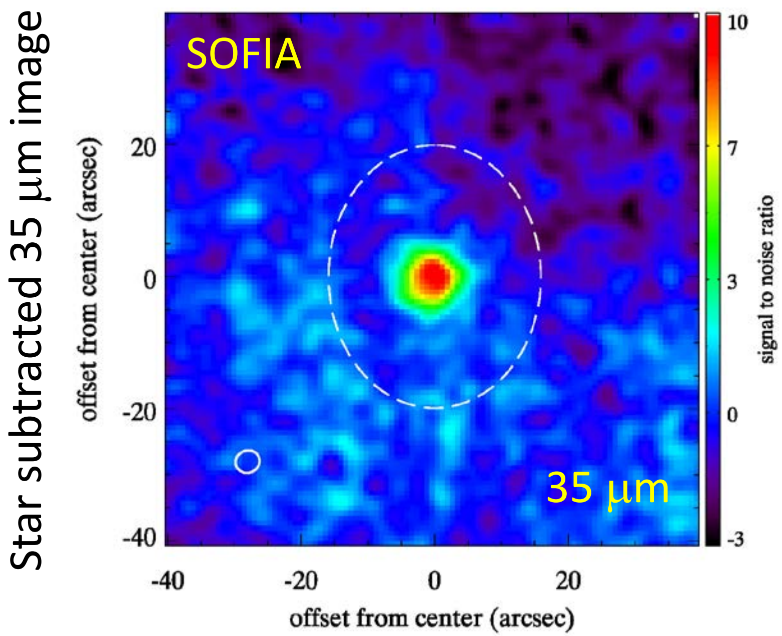

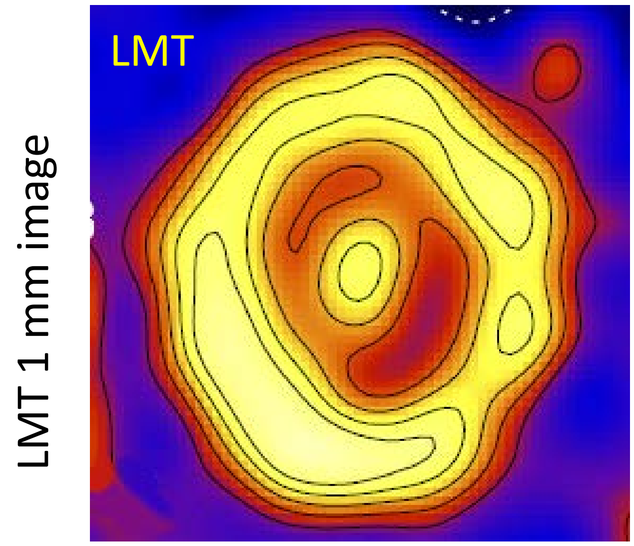

mm image shows the location of the cold belt. Chavez-Dagostino et al. 2016

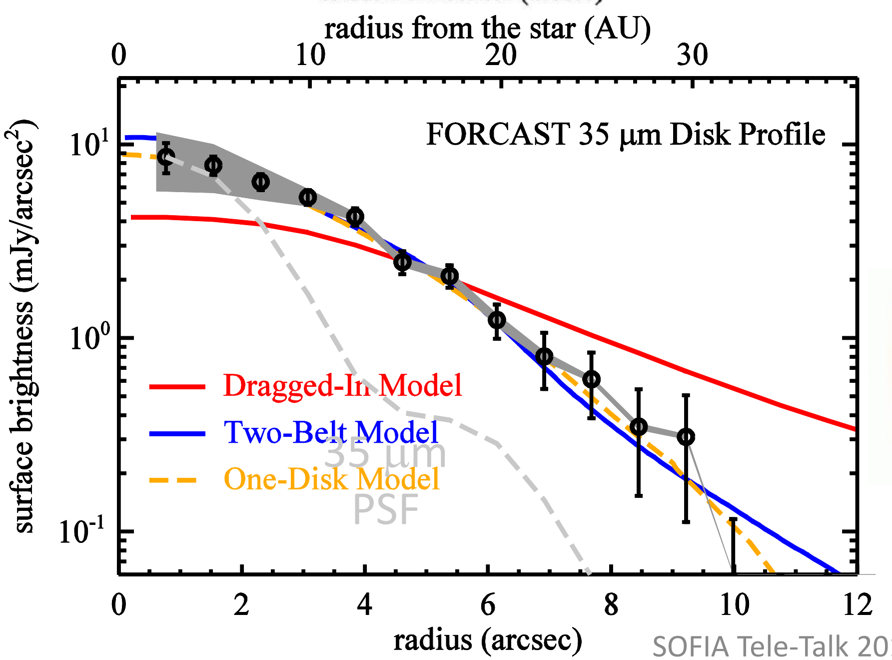

- A large amount of dragged-in grains (the parameters in Reidemeister et al. 2011) from the outer cold Kuiper-belt region is ruled out, suggesting a need of shepherding planet interior the cold belt.

- Current data cannot differentiate one broad inner disk from two narrow belts.

Future Observations of the ε Eri System

Two warm belts + One cold belt

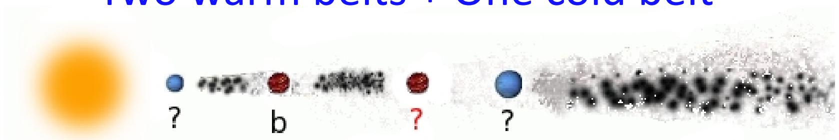

	inner warm	outer warm	Kuiper belt
R	~1.5-2 au	~ 8-12 au	~55-70 au
$\theta_{1/2}$	~0.4”-0.6”	~2.5”-3.8”	~17”-22”

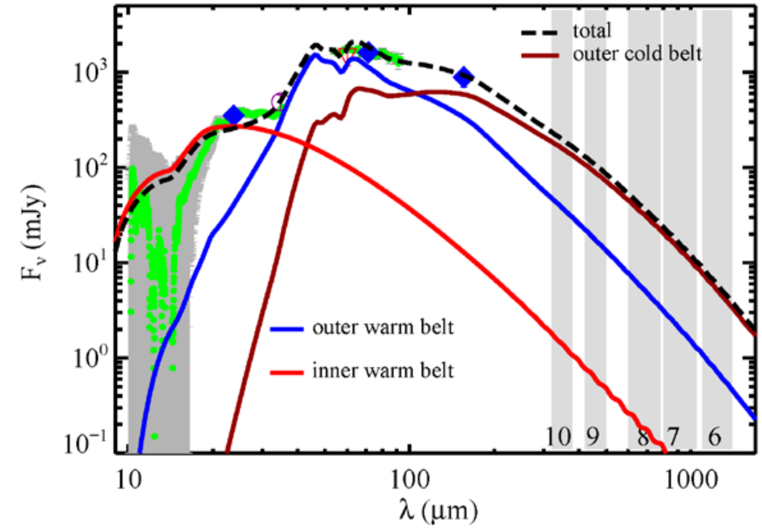

Future Observations of the ε Eri System

Two warm belts + One cold belt

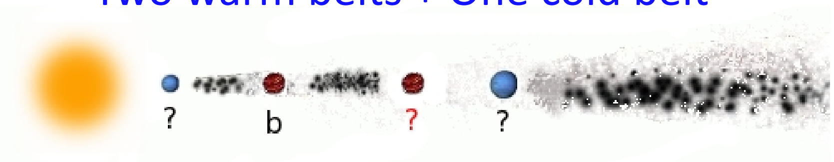

	inner warm	outer warm	Kuiper belt
R	~1.5-2 au	~ 8-12 au	~55-70 au
$\theta_{1/2}$	~0.4”-0.6”	~2.5”-3.8”	~17”-22”

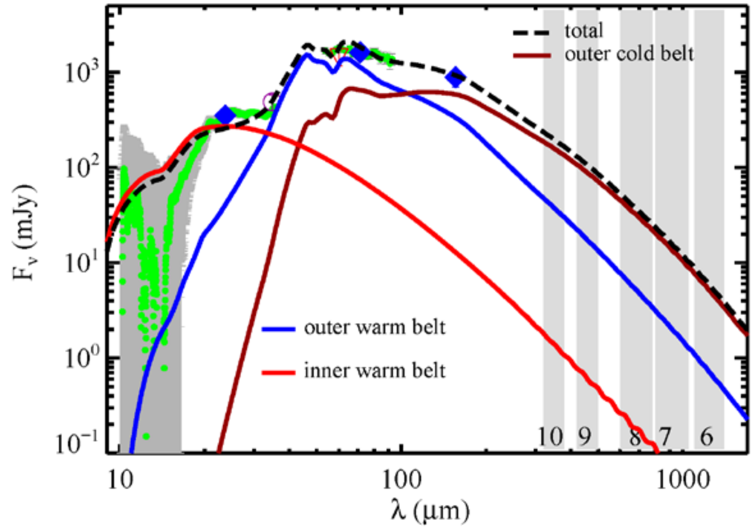

Millimeter observation consideration:

- Star is the brightest source in the millimeter wavelengths and it emission is hard to predict due to activities, i.e., resolving the dust structure from the star is the only way to firmly detect and characterize the disk.
- Surface brightness goes down as the resolvability increases

assuming an unresolved width	$F_{1.3mm}$ [mJy]	R [”]	S @ 5” beam [μJy/beam]	S @ 1” beam [μJy/beam]	S @ 0.5” beam [μJy/beam]
Kuiper belt analog	~7	20	280	56	28
outer warm belt	~1	3	……	53	26
inner warm belt	~0.02	0.5	……	……	3

Future Observations of the ε Eri System

Two warm belts + One cold belt

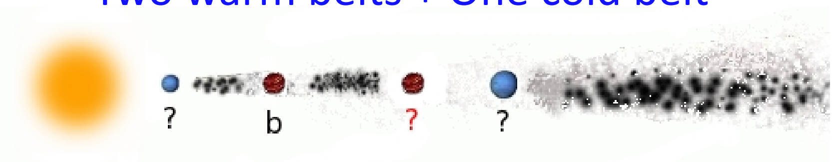

	inner warm	outer warm	Kuiper belt
R	~1.5-2 au	~ 8-12 au	~55-70 au
$\theta_{1/2}$	~0.4”-0.6”	~2.5”-3.8”	~17”-22”

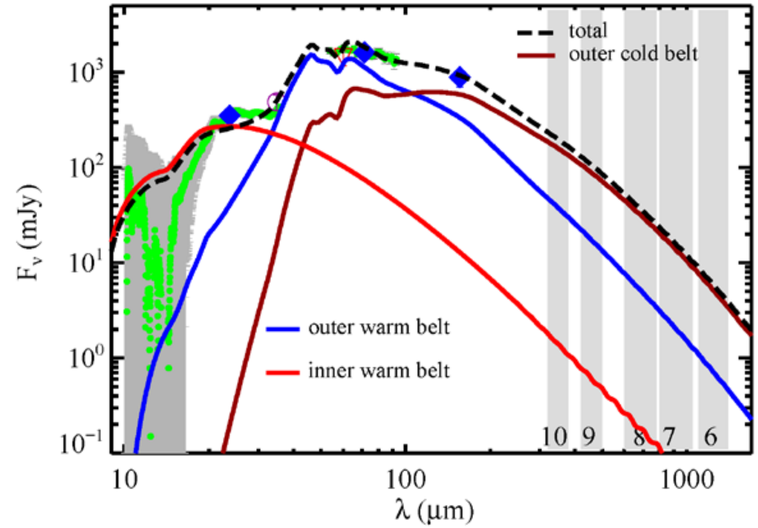

Millimeter observations consideration:

- Star is the brightest source in the millimeter wavelengths and it emission is hard to predict due to activities, i.e., resolving the dust structure from the star is the only way to firmly detect and characterize the disk.
- Disk surface brightness goes down as the resolvability increases

assuming an unresolved width	$F_{1.3mm}$ [mJy]	R [”]	S @ 5” beam [μJy/beam]	S @ 1” beam [μJy/beam]	S @ 0.5” beam [μJy/beam]
Kuiper belt analog	~7	20	280	56	28
outer warm belt	~1	3	……	53	26
inner warm belt	~0.02	0.5	……	……	3

doable in 3 hr on-source ALMA 1.3 mm obs.

very hard with mm obs.

Future Observations of the ε Eri System

Two warm belts + One cold belt

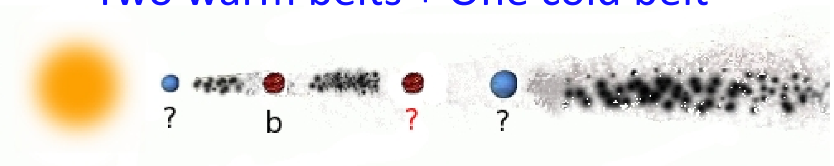

	inner warm	outer warm	Kuiper belt
R	~1.5-2 au	~ 8-12 au	~55-70 au
$\theta_{1/2}$	~0.4"-0.6"	~2.5"-3.8"	~17"-22"

JWST/MIRI: F1550C/F2300C IWA = 0.49"/2.16"
JWST/MIRI: F1500W/F2555W FWHM = 0.48"/0.82"

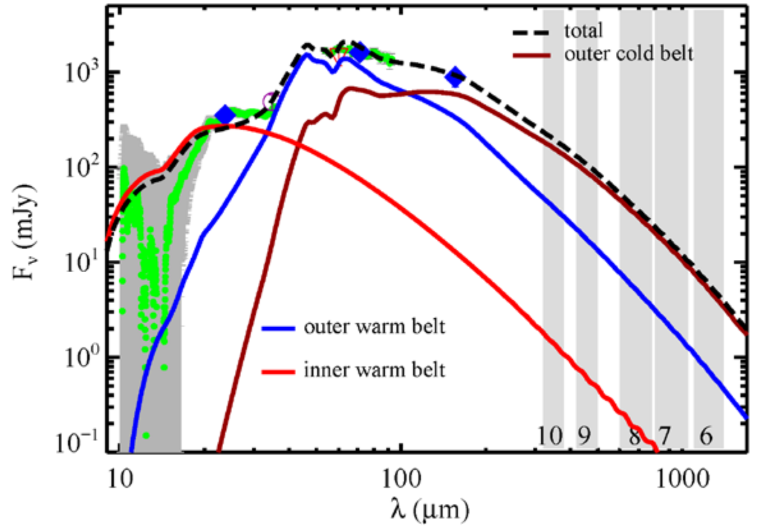

Future Observations of the ε Eri System

Two warm belts + One cold belt

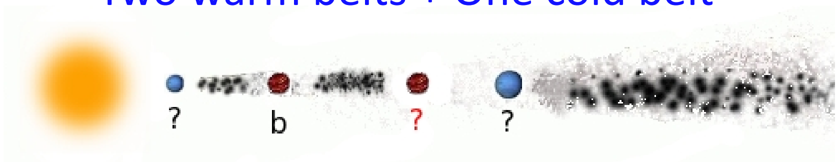

	inner warm	outer warm	Kuiper belt
R	~1.5-2 au	~ 8-12 au	~55-70 au
$\theta_{1/2}$	~0.4"-0.6"	~2.5"-3.8"	~17"-22"

JWST/MIRI: F1550C/F2300C IWA = 0.49"/2.16"
JWST/MIRI: F1500W/F2555W FWHM = 0.48"/0.82"

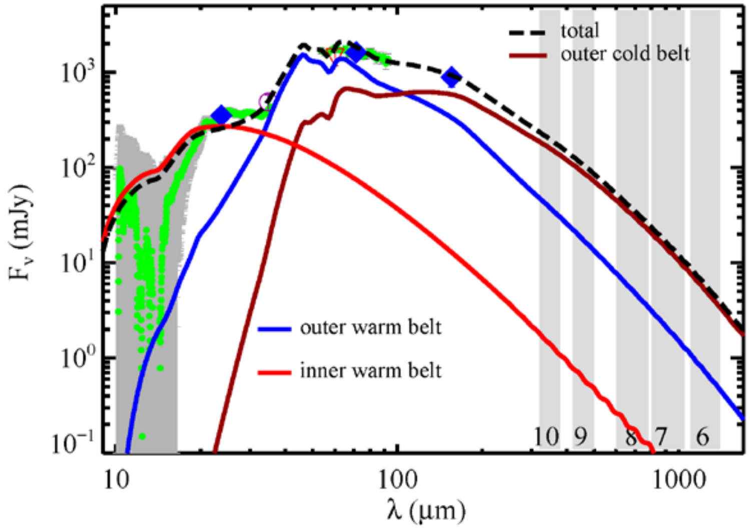

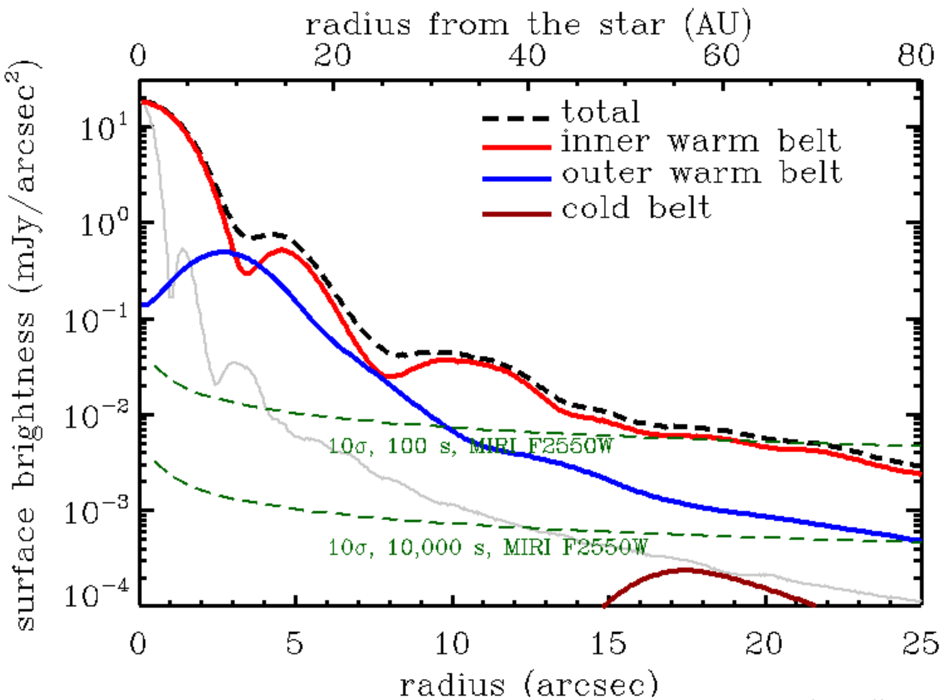

Future Observations of the ε Eri System

Two warm belts + One cold belt

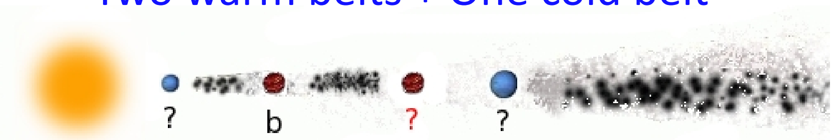

	inner warm	outer warm	Kuiper belt
R	~1.5-2 au	~ 8-12 au	~55-70 au
$\theta_{1/2}$	~0.4”-0.6”	~2.5”-3.8”	~17”-22”

JWST/MIRI: F1550C/F2300C IWA = 0.49”/2.16”

JWST/MIRI: F1500W/F2555W FWHM = 0.48”/0.82”

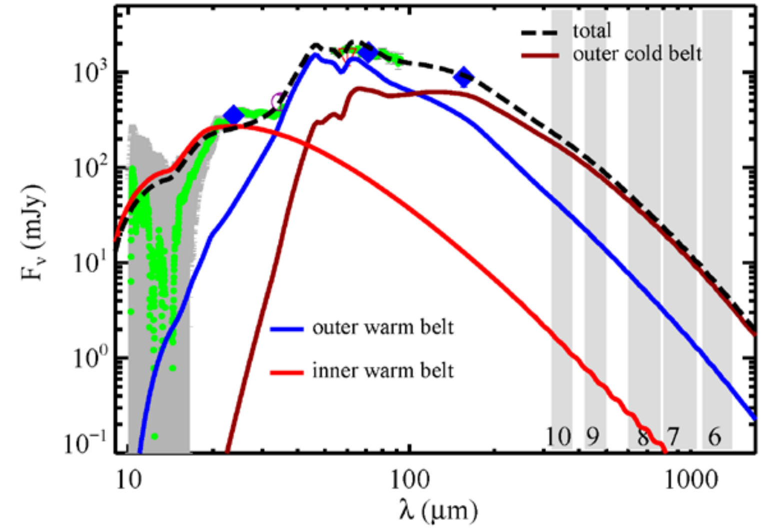

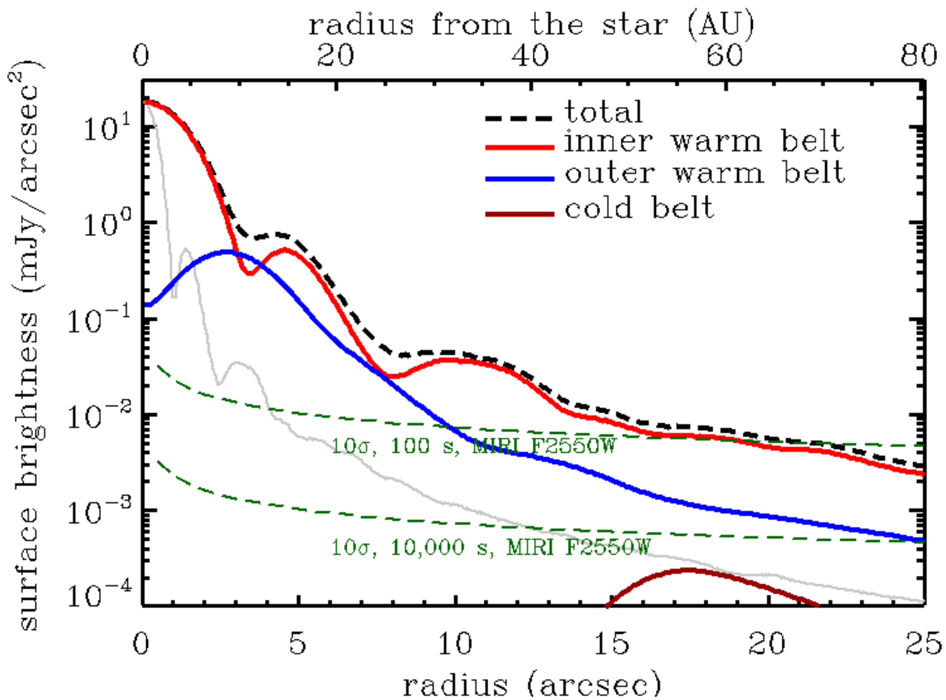

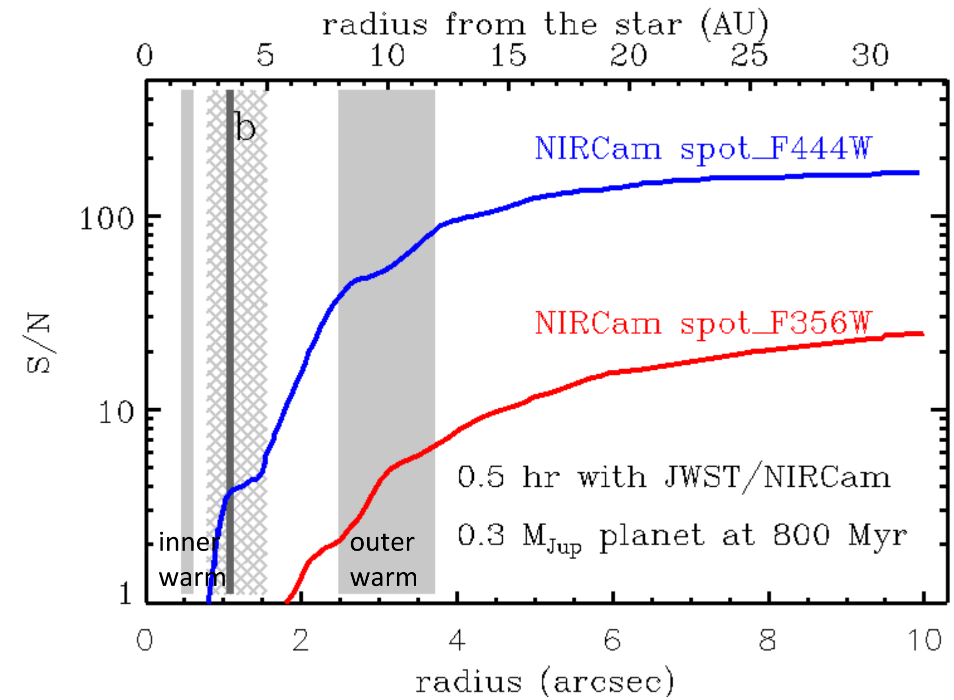

Summary

- Our SOFIA/FORCAST 35 μm image of ε Eri (1) detects a large gap between the outer cold and inner warm debris emission, and rules out the dragged-in small grains as the source of warm debris; (2) resolves the excess emission coinciding with the star, and suggests the excess emission is beyond 10 au.
- Resolved disk images at 24 and 35 μm along with the disk SED models suggest that the inner debris distribution is consistent with either a broad disk or two narrow belts with the inner one, interior of the planet ε Eri b, similar to our own asteroid belt. The latter case suggests that the ε Eri system has an architecture similar to our own solar system.